ELSEVIER

Contents lists available at ScienceDirect

Atmospheric Research

journal homepage: www.elsevier.com/locate/atmosres





Three-dimensional mapping of two coincident flashes - An upward positive flash triggered by the in-cloud activity of a downward negative flash

Fanchao Lyu^{a,b,c}, Steven A. Cummer^{d,*}, Mingli Chen^{c,**}, Zilong Qin^{c,e}, Weitao Lyu^b, Jisong Sun^{a,b}

- ^a Nanjing Joint Institute for Atmospheric Sciences, Chinese Academy of Meteorological Sciences, Nanjing, China
- ^b State Key Laboratory of Severe Weather, Chinese Academy of Meteorological Sciences, Beijing, China
- ^c Department of Building Services Engineering, The Hong Kong Polytechnic University, Hung Hom, Hong Kong, China
- ^d Electrical and Computer Engineering Department, Duke University, Durham, NC, USA
- ^e Guangdong-Hong Kong-Macao Greater Bay Area Weather Research Center for Monitoring Warning and Forecasting (Shenzhen Institute of Meteorological Innovation), Shenzhen, China

ARTICLE INFO

Keywords: Lightning 3D mapping Triggered lightning discharge Upward negative leader Upward positive flash Line charge density Lower positive charge region

ABSTRACT

Lightning mapping with radio frequency location systems plays a more and more important role in understanding the mechanism of lightning discharges during thunderstorms. Here we present a comprehensive analysis of the electromagnetic field measurements and 3-dimensional (3D) mapping of two coincident lightning flashes: an upward positive flash (+CG) with long preceding upward negative leader (UNL), which was triggered by the in-cloud (IC) activity of a nearby downward negative flash (-CG). The flashes were mapped with a low frequency (LF) mapping array deployed near Duke University and during a late-spring thunderstorm passing a plain area. The 3D LF maps show that the IC activity related to the -CG moved negative charge away from the location overhead the UNL. The UNL developed firstly upward for about 2 km and then extended horizontally for about 8 km at that height with a mean speed of 6.2×10^5 m/s. The channel line charge density of the UNL was estimated to range from $-542~\mu\text{C/m}$ to -9.21~mC/m with a mean value of -3.46~mC/m. The total positive charge transferred from the cloud to ground by the +CG flash was estimated to be about 5.8C. From the 3D maps, we inferred that the IC activity relating to the -CG flash which moved negative charge away from overhead region of the UNL could be responsible for the UNL initiation. And the existence of extensive lower positive charges further favored the long horizontal propagation of the UNL inside the cloud.

1. Introduction

Lightning discharges between cloud and ground can be classified into four types according to the propagation direction of the initiating leader and the net charge (positive or negative) transferred to ground. Investigations suggested that downward lightning flashes (initiated by either negatively or positively charged downward leaders from cloud to ground) account for more than 99% of the all the cloud-to-ground flashes (Rakov and Uman, 2003, pp. 4; Dwyer and Uman, 2013), while upward lightning flashes connected to ground are relatively uncommon.

Upward lightning flashes have been reported since McEachron (1939) and can be generally grouped into "self-initiated" flashes

(Warner et al., 2012, 2014; Zhou et al., 2012), and "other-triggered" flashes that are triggered by nearby cloud-to-ground (CG) or in-cloud (IC) lightning discharges (Wang et al., 2008; Lu et al., 2009; Warner et al., 2012; Zhou et al., 2012; Jiang et al., 2014; Saba et al., 2016). The majority of upward flashes reported to date involve the development of upward positive leaders from ground (Miki et al., 2010; Zhou et al., 2012; Warner et al., 2012; Saba et al., 2016; Yuan et al., 2017; Wu et al., 2019). The development of upward positive leaders and associated processes in artificially triggered lightning discharges has also been successfully documented with various lightning mapping systems (e.g., Dong et al., 2001; Yoshida et al., 2010; Edens et al., 2012; Warner et al., 2014). From optical measurements, visible lightning activities were detected prior to the initiation of upward positive leaders, and ground-

E-mail addresses: cummer@ee.duke.edu (S.A. Cummer), mingli.chen@polyu.edu.hk (M. Chen).

^{*} Corresponding author at: Electrical and Computer Engineering Department, Duke University, Durham, NC 27708, USA.

^{**} Corresponding author.

based lightning detection systems (e.g., National Lightning Detection Network, NLDN) also successfully documented CGs or ICs in relatively close ranges of upward leaders (Warner et al., 2014). All these suggest that the other-flash-caused charge transfer preceding an upward leader process probably play an important role in the upward leader initiation.

Comparing to upward positive leaders, only a limited number of studies on upward negative leaders from the ground have been reported, probably because of the rare occurrence of the upward positive flashes from the ground (Zhou et al., 2012; Watanabe et al., 2019). So far, studies of upward negative leaders are mainly based on measurements of channel-base currents, close electric fields, and optical images of upward flashes from high towers (e.g., Lu et al., 2009; Zhou et al., 2012; Heidler et al., 2015; Qiu et al., 2019), windmill (Wang and Takagi, 2012), a chimney (Miki et al., 2014), or rocket-triggered lightning (Pu et al., 2017), focused on the leader initiation and development below the cloud base. On the other hand, with the recent development of the lightning mapping systems, lightning 3-dimensional (3D) mapping plays a more and more important role in understanding the occurrence contexts and the dynamic development of lightning flashes, especially for in-cloud activities where no optical observations can be achieved (Rison et al., 1999; Lyu et al., 2016; Wu et al., 2018; Zhu et al., 2020). Few reports on the UNLs with lightning mapping systems were reported, and the triggering mechanisms of UNLs still need to be investigated (Rison et al., 2011; Trueblood et al., 2013; Wu et al., 2020). In a recent study, the characteristics of a few tens of UNLs observed with a low frequency fast antenna lightning mapping array during winter storms in Japan were analyzed (Wu et al., 2020). Detailed characteristics, including the UNL propagating speeds, electric field pulse shapes, comparison between these UNLs and leaders in normal lightning discharges, and the lightning activities that might be associated with the initiation of these UNLs were studied. Different types of preceding discharges might contribute to the initiation of these UNLs (Wu et al., 2020), like CG strokes, IC leaders, and some other special discharges (which produce large peak current and occur in certain special conditions). They suggested it might be because of the special and complicated charge structures during the winter thunderstorms in Japan (Zheng et al.,

Nevertheless, insights into UNLs that occurred during other usual thunderstorm environments were also crucial. The occurrence of the lightning discharge nearby an UNL, the dynamic development of an UNL inside the cloud, and the charge transfer during an UNL development from different thunderstorm circumstances, still need to be investigated with a more comprehensive observation and analysis. An effective way to achieve this is to document upward negative leaders with a lightning mapping system, which can image not only the initiation process of an UNL, but also the dynamic development of an UNL in various kinds of scenarios. It is equally essential to investigate the in-cloud activity that may link to the initiation of an UNL, which is a challenge to optical observations or channel-based current measurements, but can be well-mapped with a lightning mapping system.

Here we present the result of coordinated electromagnetic field measurements and 3D LF maps of a rare natural UNL recorded by an LF interferometric-TOA lightning mapping array (LFILMA) operated by Duke University. The 3D LF mapping result shows that this UNLinitiated +CG occurred during the time window of a normal -CG, and was probably triggered by the initial in-cloud activity of the -CG. Comparing to the UNLs reported during the winter storms in Japan, the UNL reported here was preceded by only the IC activity of the -CG that consisted of three negative return strokes following the UNL. When an UNL develops into the lower positive region of a thundercloud, the line charge density of the UNL could be much larger than that when the leader is below the thundercloud. The line charge density for the present UNL was estimated to range from $-542 \,\mu\text{C/m}$ to the maximum of -9.21mC/m as the leader developed into the thundercloud. The 3D lightning mapping and the electric charge structure of the thunderstorm suggest that the existence of the lower positive charge well and the nearby incloud activity of the -CG may play an essential role in the triggering and propagating of the UNL of the +CG.

2. Overview of the two coincident flashes and their electromagnetic field measurements

On April 20, 2015, a six-site LFILMA array (Lyu et al., 2014, 2016) (1–400 kHz, sampling rate at 1 MS/s), which contained two fixed (Duke, Hudson) and four mobile portable systems (PS1, PS2, PS3, PS4), was set up during a small cold front thunderstorm passing by Duke University. The thunderstorm arrived at our network around 22:00 (UTC) and moved out of our effective detection range around 24:00 (UTC). A total of nearly 1000 lightning events in more than 200 flashes were reported by NLDN (Cummins et al., 1998) during this time window and within 40 km from the center of the LFILMA array. The two coincident flashes studied here occurred at 22:51:37 (UTC) when the thunderstorm was over the head of the LFILMA array. Five (Duke and the other four mobile systems) of the six LF magnetic field measurement systems were running at the moment of the two flashes, which enabled us to conduct the interferometric-TOA mapping to generate a three-dimensional (3D) view of the lightning development (Lyu et al., 2014). In addition to the LF magnetic field sensors, one slow electric field change antenna (20 Hz - 400 kHz, sampling rate at 1 MS/s, and time constant of 10 ms) was also operated at Duke Forest. All measurements were synchronized by a Global Positioning System (GPS). Below we show the general view of the locations and associated meteorological contexts of these two coincident

2.1. Source locations of the two flashes in comparison with the radar observations

Fig. 1 shows the LF source locations of the two coincident flashes relative to the LFILMA array and their comparisons with the radar echoes during the two flashes. The plan view of source locations of the flashes shows that they occurred inside the network where the network location errors are less than 100 m in horizontal and 200 m in vertical. This agreed with the simulated location error patterns of a similar network configuration running graphics processing unit-based grid traverse algorithm (Qin et al., 2019). The two flashes occurred in a region where the radar reflectivity was greater than 40 dBZ and the 30 dBZ echo tops was up to 10 km high. Considering the overall strength of thunderstorms in spring there, this indicates that the thunderstorm was experiencing a relatively not weak convective process during the two flashes (Mecikalski and Carey, 2018).

2.2. Magnetic field and electric field measurements of the two coincident flashes

Fig. 2 shows the LF magnetic fields and electric field changes of the two coincident flashes measured with the sensors at Duke Forest. The whole process of the two flashes lasted for about 667 ms, started with an in-cloud initial breakdown activity in the first 87.6 ms of the flash initiation. There are four return strokes identified from the electric and magnetic field measurements, one +CG stroke followed by three -CG strokes. The electric field measurements showed a clear polarity change during the record. To some extent, this is similar to a bipolar flash that transfers two different polarities of electrical charge to ground (McEachron, 1939; Rakov, 2003). However, our 3D LF mapping (to be shown in the following section) shows that the first +CG stroke was completely spatial-separated with the either the in-cloud or the cloud-toground processes of the three -CG strokes, although their occurring times were close to each other. The 3D LF mapping provides us with more essential information for understanding the development of the flashes, especially their structures inside the clouds.

As shown in the magenta dashed box in Fig. 2, an UNL process began 87.6 ms after the IC initial activity starting and lasted for 16.3 ms,

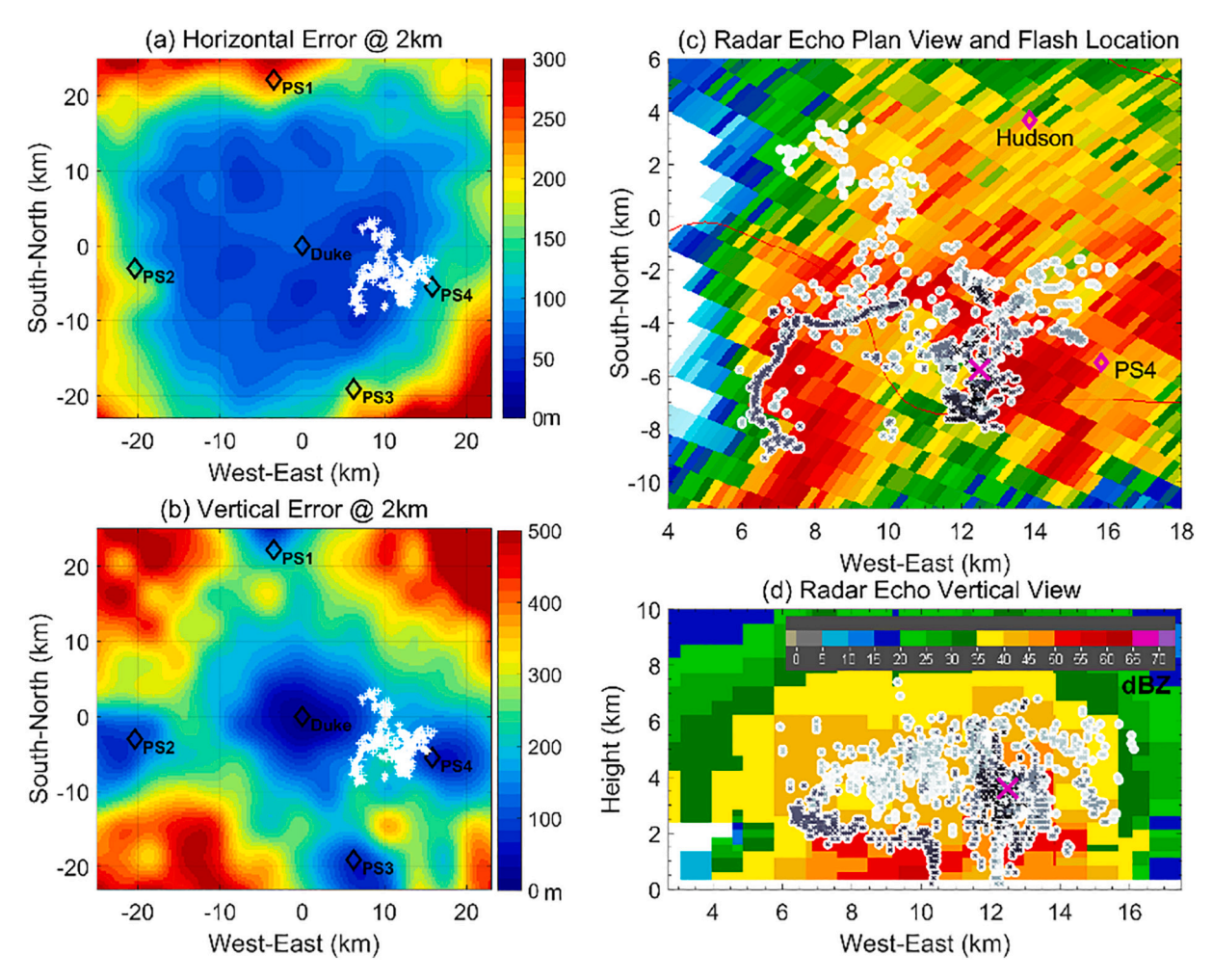


Fig. 1. Plan views of the two coincident flashes' LF source locations relative to the LFILMA array and the radar echoes of the thunderstorm. (a) and (b) are plan views of the horizontal and vertical location errors of the LFILMA network at an altitude of 2 km and the location of flash sources (white cross sign), respectively. (c) The plan view of the composite radar reflectivity at the moment of the flashes and the location of flash sources (the black and grey cross sign with white background). (d) The vertical view of the radar echoes and the flashes' source locations in west-east direction.

followed by a + CG stroke. NLDN reported a peak current of 32 KA for this +CG stroke. The first -CG stroke with a NLDN reported peak current of -12 kA occurred 78.6 ms after the +CG stroke. Two subsequent -CG strokes occurred 239.8 ms and 445.6 ms after the first -CG stroke, respectively. For some reason, both subsequent strokes were missed by NLDN, so no peak currents were reported for them. Another two IC events with a peak current of -3 kA and 3 kA, respectively, were also reported by NLDN. All these main discharge processes and NLDN reported events were marked and shown in Fig. 2.

3. The 3D radio mapping images of the two coincident flashes

The two coincident flashes were located about 15 km from the LFILMA array center, where a location error of less than 200 m in both horizontal and vertical dimensions can be achieved. Benefiting from an interferometric signal processing algorithm (Stock et al., 2014; Lyu et al., 2014), more than 2400 distinctive LF sources were mapped with the LFILMA during the 667 ms. Different processes were clearly mapped, including the IC initial breakdown process, the UNL process preceding the +CG stroke, the downward negative leader (DNL) processes before the first -CG stroke, and the dart leader (DL) processes before the two subsequent -CG strokes. Fig. 3 shows the plan view (a), vertical view (b & c), the LF source altitude versus time (e), and the LF source distribution versus altitude (d), of all the mapped LF sources.

As illustrated in Fig. 3, the flashes started with an IC initial leader at

3.6 km altitude which was propagating horizontally and downward in two main directions, as shown by the black arrowed lines marked "1" and "2". About 87.6 ms after the IC initial leader, a clear UNL process started from the ground upward. Detailed zoom-in look of this UNL showed that it seems to be initiated from a local power line tower, which might be the starting point of this UNL. The initiation position of this UNL was about 3 km horizontally away from the IC initial leader origin (the black cross). The UNL process firstly propagated vertically to about 2 km high and then extended horizontally with a total 3D length of about 10 km before the +CG stroke occurred, lasted about 16.3 ms. The +CG stroke followed the channel established by the UNL process and retraced back to ground with a NLDN reported peak current of +32 kA. During the following 78.6 ms, the IC initial leader continued but propagated in three main branches. One branch was the extension of the previous path marked "2", and two new branches started near the IC initial leader origin and followed the paths marked "3" and "4" respectively, as shown in Fig. 3(a). However, only the one following the path "2" succeeded to propagate towards ground and finally led to the first -CG stroke. This -CG stroke followed a different channel with the +CG stroke, with a ground location difference of 1.8 km. About 239.8 ms and 445.6 ms after the first -CG stroke respectively, two dart-leader/return-stroke processes were mapped. The 3D propagating speeds of the two DLs were estimated as 2×10^6 m/s and 2.7×10^6 m/s, respectively, comparable to previous measurements of CG dart leaders (Lyu et al., 2014). Both DLs followed the channel built by the downward stepped leader that led the

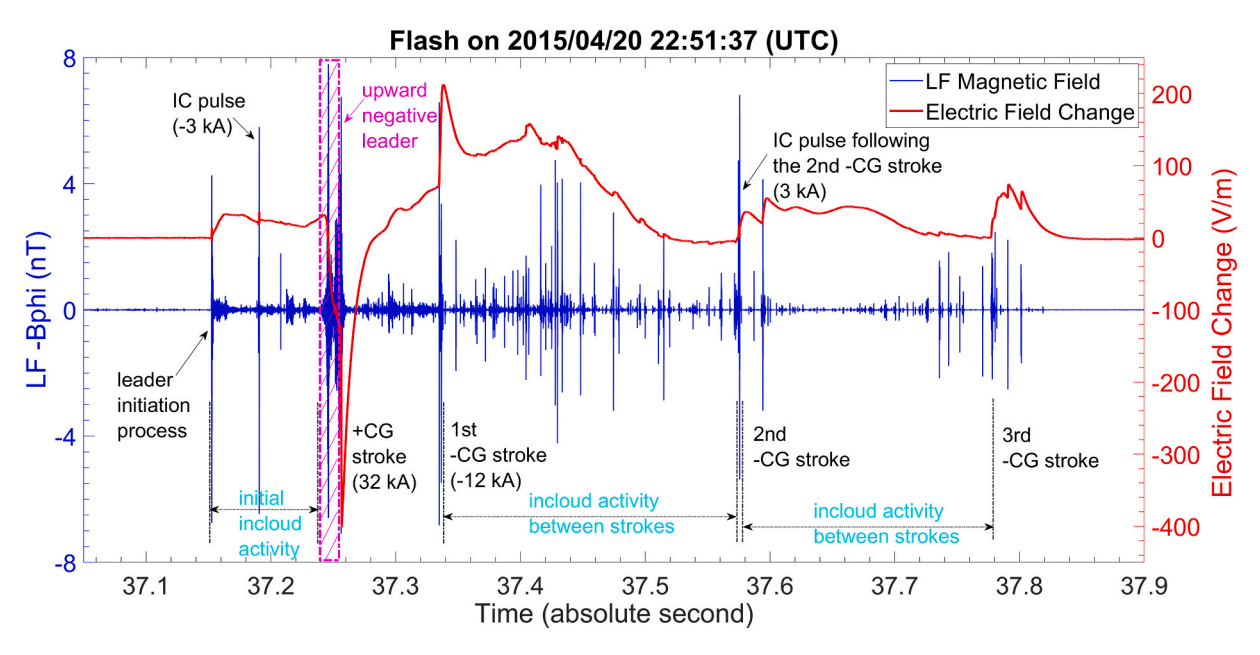


Fig. 2. The radio signals from a Duke LF magnetic field sensor and a slow electric field plate antenna of the two coincident flashes. The dashed magenta box marks the time window of the upward negative leader before the +CG stroke. Each horizontal double-sided arrow marks a specific process during the flashes. The red line is for the electric field changes and blue line is for the LF magnetic fields during the flashes, with the positive value of the electric field change indicating positive charge moving downward (or negative charge moving upward) and the negative values indicating negative charge moving downward (or positive charge moving upward). One +CG and three -CG strokes were identified from this signal record.

first -CG stroke.

It is clear from Fig. 3 that the +CG stroke and the following three -CG strokes connected to ground in two separable channels and ground locations. However, from the temporal development of the whole discharging process and 3D map, it seems that the IC activity at the initial stage of the -CG flash actually played an important role in the initiation of the UNL of the +CG flash.

4. Detailed contexts of the UNL process

Shown in Fig. 4 are the details of electric field change, LF magnetic field and LFILMA mapping results for the time period from the beginning of the IC initial leader to the end of the +CG stroke of the coincident flashes, which is a zoom-in of those in Fig. 3. It shows that the IC initial activity lasted about 87.6 ms before the initiation of the UNL (marked by "A-UNL"). The LF source location map (Fig. 4(c)) shows that the IC initial leader developed in two main branches from its origin (the magenta cross "×"), with one propagated firstly towards the south in horizontal (marked "B-1") and then upwards in vertical (marked "B-3") and another one propagated horizontally towards the north (marked "B-2"). The B-2 branch propagated towards north firstly and then went upward in the late stage, transferring negative charges probably away from the overhead region of the UNL initiation point (marked "A-UNL").

The UNL propagated about 10 km in length in 16.3 ms before the occurrence of the +CG stroke. A total of 302 LF sources were located during the UNL process. The UNL propagated almost vertically about 2 km in height in the first 2.5 ms with a speed of about 1×10^6 m/s and then extended horizontally about 8 km in length in the left time with an overall propagation speed of 6.2×10^5 m/s, both speeds well agreed with that of UNLs reported by Wu et al. (2020). The result is also consistent in general with (although a little bit larger than) previous optical measurements of UNLs (Miki et al., 2014; Heidler et al., 2015; Pu et al., 2017; Qiu et al., 2019), but was obviously faster than that of upward positive leaders (Biagi et al., 2011; Jiang et al., 2013; Wang et al., 2016; Qiu et al., 2019). During its horizontal propagating, the UNL propagated firstly towards the west for about 3.5 km and then turned to the south for about 4.5 km before the +CG stroke, produced a transient

electric field change of about 100 V/m at a distance of about 10 km on ground, and then led to a NLDN reported +CG stroke with a peak current of \pm 32 kA.

There are three LF sources mapped in a 200 μ s window just before the +CG stroke, as marked by the three black stars in Fig. 4(b)–(d). All the three sources were located at positions along the UNL channels. One was near the south ending position of the UNL channel in horizontal in cloud, and the other two were around the vertical to horizontal turning position of the UNL channel. These three sources may present the propagation of the downward positive dart leader preceding the +CG stroke along the channel built by the UNL, which corresponding to an average propagating speed of about 0.5 \times 10 8 m/s.

The UNL was the main process that was mapped with LFILMA during this period, which is probably because of the relatively stronger LF emissions from the UNL process and relatively weaker LF emissions from the IC activity during this short window of UNL. It is noted that only few (if any) branches during the UNL process were mapped. This does not necessarily mean that there were no branches during the UNL process because the LF emissions from the main leader tip were much stronger than those from the side branches.

It is noted that the UNL has propagated horizontally about 8 km long at the altitude between 2 km and 3 km inside the cloud. This may suggest that there is an extensive potential well of positive charges in the lower part of the storm, where the UNL horizontally extended for a long distance, as illustrated in a charge distribution sketch in following section. And it is also interesting to note that the UNL was propagating away from the region of the IC initial activity of the -CG flash after it penetrated in the positive charge well in lower part of the cloud. This scenario was very similar to the vertical-horizontal framework discussed by Coleman et al. (2003, 2008), and the presence of the lower positive charge well (e.g., Qie et al., 2005) was supposed to enhance the horizontal propagation of the UNL there.

5. The leader progression and charge transfer during the UNL process

Fig. 4 shows that the UNL is the dominated process in the time

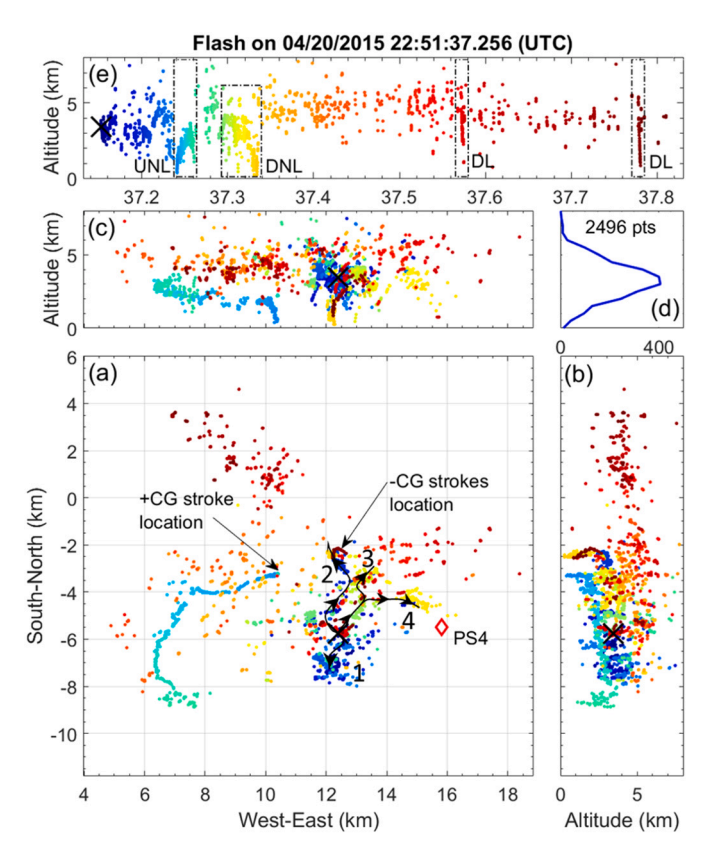


Fig. 3. LFILMA mapping images of the two coincident natural flashes on April 20, 2015, at 22:51:37 (UTC). The dot colors from blue to red in the LF source plots indicate the time variation of the flashes from start to the end. The initiation of the flashes is marked by a black cross. (a) The plan view of all located LF sources, the red diamond represents the location of the PS4 LF sensor, the +CG and three -CG stroke locations are pointed out with the arrows, and the four identifiable paths of the IC leaders are marked by the black line with arrows. (b) The vertical view of the LF sources in the direction of south to north. (c) The vertical view of the LF sources in the direction of west to east. (d) The distribution of all 2496 source points mapped versus altitude. (e) The LF sources altitude versus time during the whole lightning process, the black dashdot rectangles marked the time windows of the upward negative leader (UNL) before the +CG stroke, the downward negative leader (DNL) before the first -CG stroke, and the two dart leaders (DLs) before the two subsequent -CG strokes, respectively. (For interpretation of the references to colour in this figure legend, the reader is referred to the web version of this article.)

window from 37.24 s to 37.26 s and thus the main process that causes the electric field change during that time. Therefore, the electric field changes during that time can be used to calculate the charge transfer during the UNL process. The whole UNL process lasted about 16 ms. With the simultaneous electric field change measurements and the 3D LF source locations, the charge transferred during the UNL process can be estimated by dividing the leader channel into short sections (Chen et al., 2013).

The vertical electric field change (ΔE) produced by a short vertical channel segment (ΔH) centered at the height (H) with a line charge density (λ) at a distance (D) on ground to the measuring site, can be estimated with the equation as:

$$\Delta \mathrm{E} = rac{-2\lambda \mathrm{H}\Delta \mathrm{H}}{4\pi arepsilon_0 ig(D^2 + H^2ig)^{3/2}}.$$

where ε_0 is the permittivity of free space. And thus, the line charge density of the leader channel can be estimated from the measured electric field change when the 3D location of the short channel segment is known. It could be possible that negative upward leaders developed

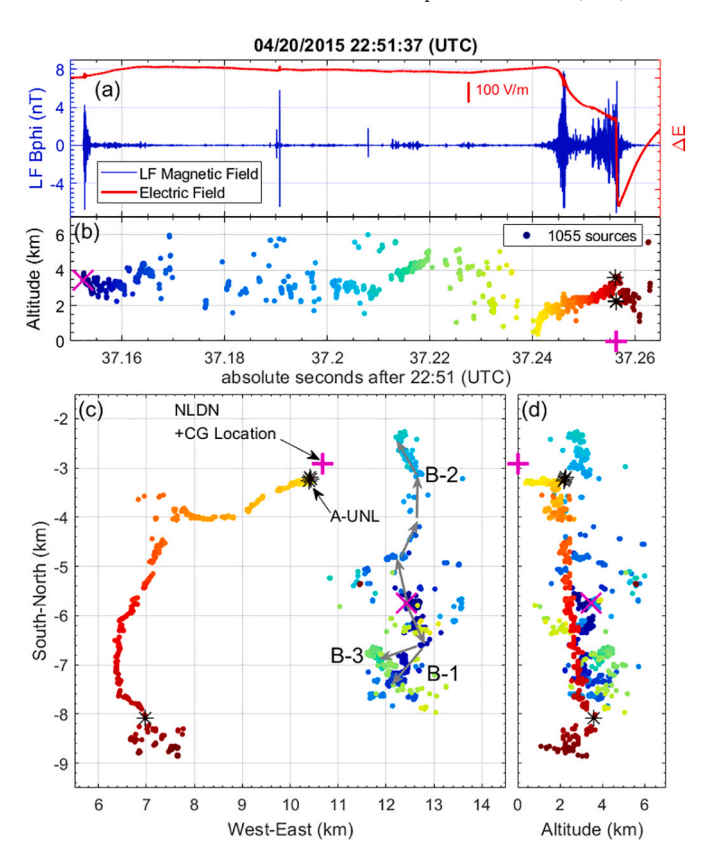


Fig. 4. Details of the LF magnetic fields, electric field changes and LF source mapping results of the IC initial leader, the UNL and +CG stroke processes, a zoom-in from Fig. 3. (a) The LF magnetic fields (blue curve) and the electric field changes (red curve) measured at Duke Forest. (b) The LF source altitude versus time for the initial IC, UNL and CG processes, the magenta cross sign "x" stands for the initiation position and the start time of the IC initial leader, magenta plus sign "+" stands for the time and NLDN location of the +CG stroke, and the three black star signs "*" are three LF sources located during a 200 µs time window just before the +CG stroke. (c) The plan view of the LF sources mapped for the initial IC, UNL and +CG processes, where the sign meanings are the same as in (b) and "B-1", "B-2" and "B-3" present the three main branches of the IC initial leader channel. (d) The vertical view of the LF sources for the IC, UNL and +CG processes in south to north direction. The color of the LF sources from blue to red presents the time variation of the IC and UNL processes during the time window from flash beginning to the end of the +CG stroke. (For interpretation of the references to colour in this figure legend, the reader is referred to the web version of this article.)

into branches during the upward propagating (Pu et al., 2017). However, from the 3D location of this UNL, there were little branches were identified, and thus it was simply considered to be a single channel leader process. The whole UNL was then separated into successive short sections by splitting the 3D located UNL channel with a 1 ms time window.

As illustrated in Fig. 5(a), based on the 1-ms time window and the LF source locations identified, the UNL channel has been divided into 15 small segments. The 3D length of the channel segment ranges from 250 m to 800 m with a mean value of 538 m. Fig. 5(b) shows the fifteen 1-ms time windows (vertical bars) and their corresponding electric field changes (red line) and channel segment center altitudes (color circles) for the UNL. It is noted that the electric field changes increased a little bit during the first three windows, which was probably because of other nearby discharge processes during the UNL initial stage. To avoid confusion, the first three windows were not involved in the line charge density calculation. Fig. 5(c) shows the length of each of the 15 channel segments (square mark) and the calculated line charge density (diamond mark, absolute value) for the segments/windows number 4 to 15. The

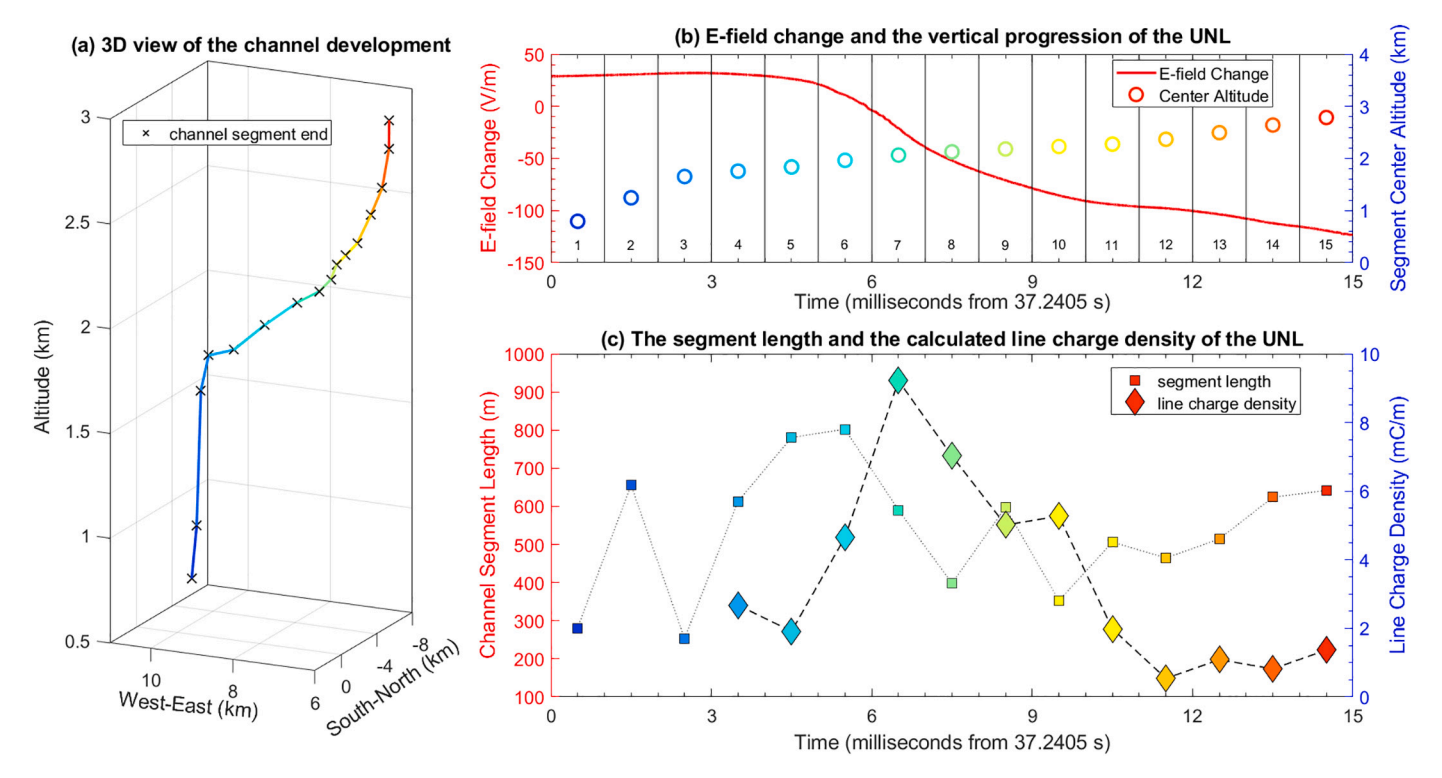


Fig. 5. The electric field changes, 3D channel development and estimated channel line charge densities for the UNL process. (a) The 3D view of the UNL channel progression, the black cross stands for the leader tip for every 1-ms time window, and the colorful line presents each short segment along the leader channel. (b) The electric field change and the center altitude of each short channel segment shown in (a). (c) The 3D length of each short channel segment shown in (a) and the calculated line charge density for each short channel segment during the UNL process. The colors of all signs in this figure present different time windows, as also shown by the time window number in (b).

line charge density ranged from $-542~\mu\text{C/m}$ to -9.21~mC/m with a mean value of -3.46~mC/m, with the peak appeared on the segment number 7 at 2.1 km high above the ground. The peak value of the line charge density at the height of 2.1 km may be because of the existence of a local positive charge well, which can also be seen from the energetic LF magnetic pulses shown in Fig. 4(a) and the scattered 3D locations shown in Fig. 4(b), around this time and position. The line charge density decreased from the peak value of -9.21~mC/m to about -1~mC/m in about 10 ms as the UNL moved from segment number 7 to 15. While the leader moved upward only from 2.1 km to 2.3 km in height, it moved horizontally about 8 km long, suggesting the existence of an extensive positive charge well there.

The whole +CG stroke following the UNL transferred about 5.8C of positive charge to ground in 1 ms of its occurrence, with an estimated charge moment change of 16.5C-km. Considering the UNL process only, a total of 3.5C positive charges was transferred to ground before the +CG stroke occurrence. The estimated line charge density for the present UNL is reasonably consistent with the averaged line charge density estimated for UNLs in upward positive flashes from high towers (Heidler et al., 2015) and chimney (Miki et al., 2014), but is several times larger than that of low altitude upward negative leader in rocket-triggered lightning (Pu et al., 2017) and that of upward positive leaders in rocket-triggered lightning (Chen et al., 2013). The UNL from the rockettriggered lightning (Pu et al., 2017) involved only initial continuous currents without return strokes followed, and had a smaller charge transfer than the present UNL. It is interesting to note that the line charge density of the present UNL is comparable to that of the negative stepped leaders in IC discharges (Proctor, 1997), and downward positive leaders which connected with high buildings on ground (Gao et al., 2020). This may be due to that the most of channel of the present UNL were developed inside the thundercloud, and thus a large amount of charges were involved in the leader's long horizontal extension.

6. The thunderstorm charge structure and morphology of the \mbox{UNL}

Atmospheric sounding data was measured at Greensboro, North Carolina, which was about 78 km from the thunderstorm in this study. This is the closest available atmospheric sounding data to the thunderstorm. Although it was not that close to the thunderstorm, it still provided useful background information for the temperature layer of nearby regions. The data showed that the 0 °C layer was at the height of about 3.1 km above ground and the 0 °C to $-15\,^{\circ}\mathrm{C}$ layer (the main negative charge region in a thunderstorm with the peak at $-5\,^{\circ}\mathrm{C}$) was in the range of 3.1 km to 5.6 km high above ground. While the lower temperature layer of $-19\,^{\circ}\mathrm{C}$ to $-40\,^{\circ}\mathrm{C}$, which is supposed to be the main positive charge region in a thunderstorm with the peak at $-25\,^{\circ}\mathrm{C}$, was in the range of 6 km to 9 km high above ground.

Fig. 6(a) shows the altitude distribution of 52,560 LF source locations mapped for more than 60 flashes in a 14-min time window centered at the time of the UNL in this study. The distribution of these lightning discharge source locations could reflect the potential wells of charges associated with these discharge sources (Coleman et al., 2003, 2008; Zheng et al., 2019), and thus reflect the thunderstorm charge layer structures. There are three main peaks in the LF source distribution, appeared at the altitudes of 1.8 to 2.5 km, 2.5 to 5.5 km, and 5.5 to 9 km, respectively. Note that the vertical distribution of the charges from the LF sources distribution agreed well with the atmospheric sounding shown above. The development and propagation of lightning leaders could be connected to local potential charge distributions (Williams, 1989; Coleman et al., 2003, 2008; Wiens et al., 2005). Fig. 6(a) suggests that the present thunderstorm may have a typical three-layer charge structure: a lower positive charge region centered at about 2 km height, a middle main negative charge region centered at about 4 km height, and an upper positive charge region centered at about 7 km height. The evident lower positive charge region at about 2 km height can also be

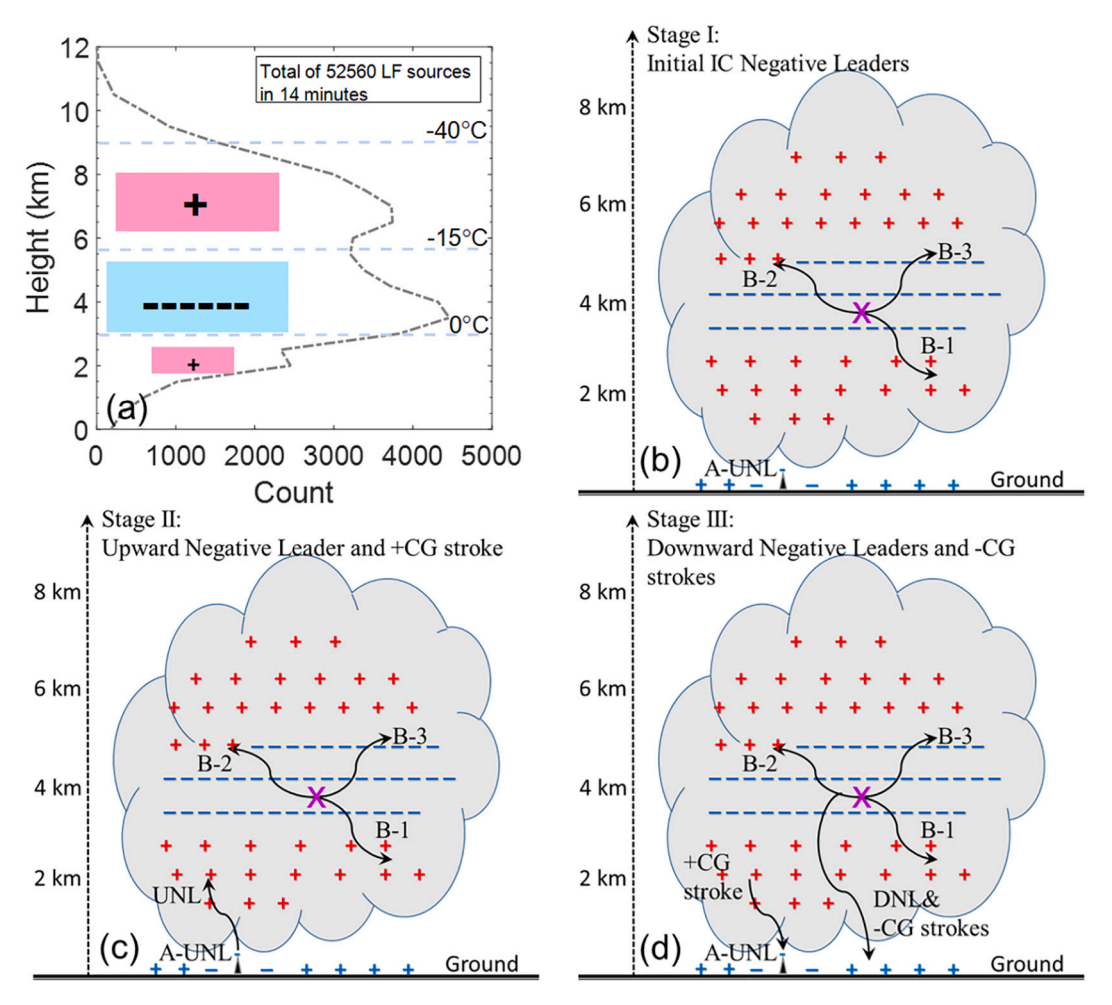


Fig. 6. The charge structure inferred from the sounding data and LF source location distribution of the thunderstorm (a), and the illustration of the three development stages (b, c, and d) of the coincident flashes including the IC activity, the UNL, one +CG stroke and three -CG strokes. The horizontal axis illustrates the relative horizontal distance, while the vertical axis marks the altitude of the inferred charge structure and the lightning discharges.

inferred from the long horizontal channel extension of the UNL prior to the +CG stroke (Coleman et al., 2003, 2008).

Based on the inferred thunderstorm charge layer structure in Fig. 6 (a) and the 3D lightning LF source maps with clear leader branches propagation, we have separated the development of the two coincident flashes into three main stages, as illustrated in Fig. 6(b) to (d):

Stage I: The initiation and development of the IC activity, which were dominated by the negative initial IC leaders between the main negative charge layer and the lower positive charge layer. In the first 86 ms of the flashes, the downward negative IC leader between the main negative and lower positive charge region branched into different directions, as marked by the black arrow lines in Fig. 4(a) and the schematic graph in Fig. 6(b) to (d).

Stage II: The negative IC leader developed into three main branches, with two propagated horizontally and one vertically away from overhead position of the following UNL. They were supposed to bring negative charges away from the overhead region of the UNL, and thus increased the local positive polarity electric field (atmospheric electricity sign convention) that favored the triggering of the UNL. Meanwhile, the existence of the lower positive charge well facilitated the long in-cloud horizontal propagation of the UNL followed by the +CG stroke.

Stage III: The development of the stepped leader associated with the first -CG stroke and the following two subsequent -CG strokes. After the +CG stroke, the IC activity continued and developed into different branches, with one of them successfully propagated downward to ground and ended with the first -CG stroke. After that, the IC activity

further developed and resulted in two negative dart leader/ return stroke processes.

The three main stages of the two coincident flashes were intrinsically dependent, as illustrated by the LF source mapping results. The existence of the lower positive charge region favored the initiation of the UNL from the power line tower (Jiang et al., 2014). The initial IC activity, which moved negative charges away from overhead region of the UNL, enhanced the local positive electric field that further favored the initiation of the UNL.

There are many other reports of upward positive or negative lightning leaders triggered by nearby in-cloud activity (Wang et al., 2008; Lu et al., 2009; Zhou et al., 2012; Heidler et al., 2015). Wu et al. (2020) reported a few tens of UNLs triggered by nearby negative stroke, stroke-like processes and sometimes IC discharges, in the complicated winter storms in Japan. The present study provided a further clear picture, with the LFILMA mapping system from both temporal and spatial views, of the relationship between the IC activity, the UNL, the +CG stroke, three –CG strokes in two coincident flashes, and the thunderstorm charge structure.

Many previous studies suggested that proper magnitude of the lower positive charge could be an effective driver of the formation of the downward negative leader and will facilitate the downward propagation of the negative leader to terminate as an –CG flash (Clarence and Malan, 1957; Qie et al., 2005; Coleman et al., 2008; Nag and Rakov, 2009). Although, a large amount of lower positive charge would prevent the downward propagation of negative leaders to ground, which finally

ended as inverted IC flashes. We indicated that the existence of the lower positive charge region and the IC activity with proper moving directions could facilitate the initiation of upward negative leaders from the objects on ground, and further enable the horizontal propagation of the negative leaders in cloud.

7. Summary

In this study, using a combination of a slow electric field change antenna, a LF magnetic field sensor and a 3D LF lightning mapping array, we have carried out a comprehensive analysis of two coincident lightning flashes that involved a rare case of upward negative leader. The electric and magnetic field records showed that two flashes overlapped in time, with one a +CG flash and one a -CG flash. The 3D LF mapping showed that the two flashes were spatially unconnected but intrinsically dependent. The +CG stroke was proceeded by an UNL triggered by the nearby IC activity relating to the following -CG strokes, although the +CG stroke and the -CG strokes connected ground with different channels. The UNL analyzed in this study was produced in a late-spring thunderstorm circumstance over a plain area of North America. Comparing to the recently reported UNLs observed during the winter thunderstorms in Japan, our results with the LFILMA mapping system from both temporal and spatial views showed the occurrence of UNL in a more usual thunderstorm environment. And thus, both draw crucial pieces of the picture on the understanding of UNL's production.

The UNL produced strong LF radio emissions and had an average speed of 6.2×10^5 m/s when it propagated inside the cloud, which is a typical speed of downward negative leaders. The line charge density along the UNL channel was estimated to range from $-542~\mu\text{C/m}$ to -9.21~mC/m with a mean value of -3.46~mC/m, while the total positive charge transferred to ground by the UNL process was estimated to be about +3.5C. The total positive charge transferred to ground by the +CG stroke following the UNL was estimated to be about +5.8C. The speed of the positive dart leader that preceding the +CG stroke and following the UNL-built channel was estimated to be about $0.5 \times 10^8~\text{m/s}$.

The two flashes were observed during a storm that had a relatively low vertical extension with a typical three-layer charge structure: a lower positive region around 2 km height, a main negative region around 4 km height, and an upper positive charge region around 7 km height. We inferred that it is the existence of the lower positive charge region and the nearby IC negative leaders propagating away from the UNL overhead location that favored the initiation of this unusual UNL. And the extensive lower positive charge region further facilitated the long horizontal propagation of the UNL inside the cloud.

Declaration of Competing Interest

The authors declare that they have no known competing financial interests or personal relationships that could have appeared to influence the work reported in this paper.

Acknowledgements

The authors would like to acknowledge supports from the National Science Foundation Dynamic and Physical Meteorology program (grant AGS-1565606), the Defense Advanced Research Projects Agency (DARPA) Nimbus program (grant HR0011-10-1-0059), the Open Grants of the State Key Laboratory of Severe Weather of China (grant 2020LASW-A02), and the Research Grant Council of Hong Kong (grants 15214719 and 15215120). The original work presented in this study was started when F. Lyu worked at Duke University.

References

Biagi, C.J., Uman, M.A., Hill, J.D., Jordan, D.M., 2011. Observations of the initial, upward-propagating, positive leader steps in a rocket-and-wire triggered lightning

- discharge. Geophys. Res. Lett. 38 (24), L24809 https://doi.org/10.1029/2011gl049944.
- Chen, M., Zheng, D., Du, Y., Zhang, Y., 2013. Evolution of line charge density of steadily developing upward positive leaders in triggered lightning. J. Geophysical. Res. Atmos. 118, 4670–4678. https://doi.org/10.1002/jgrd.50446.
- Clarence, N.D., Malan, D.J., 1957. Preliminary discharge processes in lightning flashes to ground. O. J. R. Meteorol. Soc. 83, 161–172.
- Coleman, L.M., Marshall, T.C., Stolzenburg, M., Hamlin, T., Krehbiel, P.R., Rison, W., Thomas, R.J., 2003. Effects of charge and electrostatic potential on lightning propagation. J. Geophys. Res. 108 (D9), 4298. https://doi.org/10.1029/ 2002/ID002718
- Coleman, L.M., Stolzenburg, M., Marshall, T.C., Stanley, M., 2008. Horizontal lightning propagation, preliminary breakdown, and electric potential in New Mexico thunderstorms. J. Geophys. Res. 113, D09208 https://doi.org/10.1029/ 2007.ID009459
- Cummins, K.L., Murphy, M.J., Bardo, E.A., Hiscox, W.L., Pyle, R.B., Pifer, A.E., 1998. A combined TOA/MDF technology upgrade of the U.S. National Lightning Detection Network. J. Geophys. Res. 103 (D8), 9035–9044. https://doi.org/10.1029/ 98JD00153.
- Dong, W., Liu, X., Yu, Y., Zhang, Y., 2001. Broadband interferometer observations of a triggered lightning. Chin. Sci. Bull. 46 (18), 1561–1565. https://doi.org/10.1007/ BF02900582.
- Dwyer, J.R., Uman, M.A., 2013. The physics of lightning. Phys. Rep. https://doi.org/ 10.1016/j.physrep.2013.09.004.
- Edens, H.E., et al., 2012. VHF lightning mapping observations of a triggered lightning flash. Geophys. Res. Lett. 39, L19807 https://doi.org/10.1029/2012GL053666.
- Gao, Y., Chen, M., Qin, Z., Lyu, W., Qi, Q., Du, Y., Zhang, Y., 2020. Leader charges, currents, ambient electric fields and space charges along downward positive leader paths retrieved from ground measurements in metropolis. J. Geophys. Res. Atmos. 125 https://doi.org/10.1029/2020JD032818 e2020JD032818.
- Heidler, F.H., Manhardt, M., Stimper, K., 2015. Characteristics of upward positive lightning initiated from the Peissenberg tower, Germany. IEEE Trans. Electromagn. Compat. 57 (1), 102–111. https://doi.org/10.1109/TEMC.2014.2359584.
- Jiang, R., Qie, X., Wang, C., Yang, J., 2013. Propagating features of upward positive leaders in the initial stage of rocket-triggered lightning. Atmos. Res. 129–130, 90–96. https://doi.org/10.1016/j.atmosres.2012.09.005.
- Jiang, R., Qie, X., Wu, Z., Wang, D., Liu, M., Lu, G., Liu, D., 2014. Characteristics of upward lightning from a 325 m tall meteorology tower. Atmos. Res. 149, 111–119. https://doi.org/10.1016/j.atmosres.2014.06.007.
- Lu, W., Wang, D., Zhang, Y., Takagi, N., 2009. Two associated upward lightning flashes that produced opposite polarity electric field changes. Geophys. Res. Lett. 36, L05801 https://doi.org/10.1029/2008GL036598.
- Lyu, F., Cummer, S.A., Solanki, R., Weinert, J., McTague, L., Katko, A., Barrett, J., Zigoneanu, L., Xie, Y., Wang, W., 2014. A low-frequency near-field interferometric-TOA 3-D Lightning Mapping Array. Geophys. Res. Lett. 41, 7777–7784. https://doi. org/10.1002/2014GI.061963.
- Lyu, F., Cummer, S.A., Lu, G., Zhou, X., Weinert, J., 2016. Imaging lightning intracloud initial stepped leaders by low-frequency interferometric lightning mapping array. Geophys. Res. Lett. 43 https://doi.org/10.1002/2016GL069267.
- McEachron, K.B., 1939. Lightning to the empire state building. J. Frankl. Inst. 227, 149–217. https://doi.org/10.1016/S0016-0032(39)90397-2.
- Mecikalski, R.M., Carey, L.D., 2018. Radar reflectivity and altitude distributions of lightning flashes as a function of three main storm types. J. Geophys. Res. 123, 12,814–12,828. https://doi.org/10.1029/2018JD029238.
- Miki, M., Miki, T., Wada, A., Asakawa, A., Asuka, Y., Honjo, N., 2010. Observations of Lightning Flashes to Wind Turbines, Paper Presented at the 30th International Conference on Lightning Protection, Cagliari, Italy.
- Miki, M., Miki, T., Asakawa, A., Shindo, T., 2014. Characteristics of Negative Upward Stepped Leaders in Positive Upward Lightning, Paper Presented at XV International Conference on Atmospheric Electricity.
- Nag, A., Rakov, V.A., 2009. Some inferences on the role of lower positive charge region in facilitating different types of lightning. Geophys. Res. Lett. 36, L05815 https:// doi.org/10.1029/2008GL036783.
- Proctor, D., 1997. Lightning flashes with high origins. J. Geophys. Res. 102 (D2), 1693–1706. https://doi.org/10.1029/96JD02635.
- Pu, Y., Jiang, R., Qie, X., Liu, M., Zhang, H., Fan, Y., Wu, X., 2017. Upward negative leaders in positive triggered lightning: Stepping and branching in the initial stage. Geophys. Res. Lett. 44, 7029–7035. https://doi.org/10.1002/2017GL074228.
- Qie, X., Zhang, T., Chen, C., Zhang, G., Zhang, T., Wei, W., 2005. The lower positive charge center and its effect on lightning discharges on the Tibetan plateau. Geophys. Res. Lett. 32, L05814 https://doi.org/10.1029/2004GL022162.
- Qin, Z., Chen, M., Lyu, F., Cummer, S.A., Zhu, B., Liu, F., Du, Y.-p., 2019. A GPU-based grid traverse algorithm for accelerating lightning geo-location process. IEEE Trans. Electromagn. Compat. https://doi.org/10.1109/TEMC.2019.2907715.
- Qiu, Z., Yang, Y., Qin, Z., Chen, M., Lyu, F., Guo, H., et al., 2019. Optical and current measurements of lightning attachment to the 356-m-high Shenzhen Meteorological Gradient Tower in Southern Coastal Area of China. IEEE Access 7, 155372–155380. https://doi.org/10.1109/ACCESS.2019.2949127.
- Rakov, V.A., 2003. A review of positive and bipolar lightning discharges. Bull. Am. Meteorol. Soc. 84 (6), 767–776.
- Rakov, V.A., Uman, M.A., 2003. Lightning: Physics and Effects. Cambridge Univ. Press, Cambridge, U. K.
- Rison, W., Thomas, R.J., Krehbiel, P.R., Hamlin, T., Harlin, J., 1999. A GPS-based threedimensional lightning mapping system: initial observations in central New Mexico. Geophys. Res. Lett. 26, 3573–3576.

- Rison, W., Krehbiel, P.R., Stock, M., Godman, H., Lu, G., Cummer, S.A., 2011.
 Observations of a Naturally-triggered Upward-initiated Positive CG Lightning Flash,
 Paper Presented at American Geographical Union Fall Meeting, #AE13A02.
- Saba, M.M.F., Schumann, C., Warner, T.A., Ferro, M.A.S., de Paiva, A.R., Helsdon Jr., J., Orville, R.E., 2016. Upward lightning flashes characteristics from highspeed videos. J. Geophys. Res. Atmos. 121, 8493–8505. https://doi.org/10.1002/2016JD025137.
- Stock, M.G., Akita, M., Krehbiel, P.R., Rison, W., Edens, H.E., Kawasaki, Z., Stanley, M. A., 2014. Continuous broadband digital interferometry of lightning using a generalized cross-correlation algorithm. J. Geophys. Res. Atmos. 119, 3134–3165. https://doi.org/10.1002/2013JD020217.
- Trueblood, J., Eack, K., Winn, W.P., Edens, H.E., Aulich, G.D., Eastvedt, E.M., Petersen, D., Stock, M., Lapierre, J.L., Sonnenfeld, R.G., 2013. Triggered Upward Negative Lightning Leaders, Paper Presented at American Geographical Union Fall Meeting, Abstract #AE12A07.
- Wang, D., Takagi, N., 2012. Three unusual upward positive lightning triggered by other nearby lightning discharge activity. In: Paper presented at the 22nd International Lightning Detection Conference, Broomfield, CO, USA, 2012.
- Wang, D., Takagi, N., Watanabe, T., Sakurano, H., Hashimoto, M., 2008. Observed characteristics of upward leaders that are initiated from a windmill and its lightning protection tower. Geophys. Res. Lett. 35, L02803 https://doi.org/10.1029/ 2007c1.032136
- Wang, Z.C., Qie, X.S., Jiang, R.B., Wang, C.X., Lu, G.P., Sun, Z.L., Liu, M.Y., Pu, Y.J., 2016. High-speed video observation of stepwise propagation of a natural upward positive leader. J. Geophys. Res. Atmos. 121 (24), 14307–14315. https://doi.org/ 10.1002/2016.ID025605.
- Warner, T.A., Cummins, K.L., Orville, R.E., 2012. Upward lightning observations from towers in Rapid City, South Dakota and comparison with National Lightning Detection Network data, 2004–2010. J. Geophys. Res. 117, D19109 https://doi.org/ 10.1029/2012.ID018346.
- Warner, T.A., Lang, T.J., Lyons, W.A., 2014. Synoptic scale outbreak of self-initiated upward lightning (SIUL) from tall structures during the central U.S. blizzard of 1–2 February 2011. J. Geophys. Res. Atmos. 119, 9530–9548. https://doi.org/10.1002/ 2014.JD021691.
- Watanabe, N., Nag, A., Diendorfer, G., Pichler, H., Schulz, W., Rakov, V.A., Rassoul, H.K., 2019. Characteristics of currents in upward lightning flashes initiated from the

- Gaisberg Tower. IEEE Trans. Electromagn. Compat. 61 (3), 705–718. https://doi.org/10.1109/TEMC.2019.2916047.
- Wiens, K.C., Rutledge, S.A., Tessendorf, S.A., 2005. The 29 June 2000 supercell observed during STEPS. part II: lightning and charge structure. J. Atmos. Sci. 62 (12), 4151–4177.
- Williams, E.R., 1989. The tripole structure of thunderstorms. J. Geophys. Res. 94, 13.151–13.167.
- Wu, T., Wang, D., Takagi, N., 2018. Lightning mapping with an array of fast antennas. Geophys. Res. Lett. 45, 3698–3705. https://doi.org/10.1002/2018GL077628.
- Wu, B., Lyu, W., Qi, Q., Ma, Y., Chen, L., Zhang, Y., et al., 2019. Synchronized two-station optical and electric field observations of multiple upward lightning flashes triggered by a 310-kA +CG flash. J. Geophys. Res. 124, 1050–1063. https://doi.org/10.1029/2018JD029378.
- Wu, T., Wang, D., Takagi, N., 2020. Upward negative leaders in positive upward lightning in winter: propagation velocities, electric field change waveforms, and triggering mechanism. J. Geophys. Res. 125 https://doi.org/10.1029/ 2020JD032851 e2020JD032851.
- Yoshida, S., Biagi, C.J., Rakov, V.A., Hill, J.D., Stapleton, M.V., Jordan, D.M., Uman, M. A., Morimoto, T., Ushio, T., Kawasaki, Z.-I., 2010. Three-dimensional imaging of upward positive leaders in triggered lightning using VHF broadband digital interferometers. Geophys. Res. Lett. 37, L05805 https://doi.org/10.1029/2009GL042065.
- Yuan, S., Jiang, R., Qie, X., Wang, D., Sun, Z., Liu, M., 2017. Characteristics of upward lightning on the Beijing 325 m meteorology tower and corresponding thunderstorm conditions. J. Geophys. Res. 122, 12,093–12,105. https://doi.org/10.1002/ 2017 ID022198
- Zheng, D., Wang, D., Zhang, Y., Wu, T., Takagi, N., 2019. Charge regions indicated by LMA lightning flashes in Hokuriku's winter thunderstorms. J. Geophys. Res. 124, 7179–7206. https://doi.org/10.1029/2018JD030060.
- Zhou, H., Diendorfer, G., Thottappillil, R., Pichler, H., Mair, M., 2012. Measured current and close electric field changes associated with the initiation of upward lightning from a tall tower. J. Geophys. Res. 117, D08102 https://doi.org/10.1029/ 2011 D017269
- Zhu, Y., Bitzer, P., Stewart, M., Podgorny, S., Corredor, D., Burchfield, J., et al., 2020. Huntsville Alabama Marx Meter Array 2: upgrade and capability. Earth Space Sci. 7 https://doi.org/10.1029/2020EA001111 e2020EA001111.